

Stability and variability of the thermohaline circulation in the past and future: a study with a coupled model of intermediate complexity

Andrey Ganopolski, Stefan Rahmstorf

Potsdam Institute for Climate Impact Research, Potsdam, Germany

We present the results of a study of the stability properties of the thermohaline ocean circulation (THC) and the possible mechanisms of rapid climate changes using the climate system model of intermediate complexity, CLIMBER-2. We consider two climate states, the warm modern climate and the cold glacial climate, and compare the stability properties of the THC in both cases. While for modern climate there are two stable circulation modes: the “warm” and the “off” mode, under glacial conditions we find only one (“cold”) stable mode of Atlantic ocean circulation. This mode is characterized by deep water formation south of Iceland and has a shallower overturning with weaker outflow to the southern Atlantic. Another mode of the THC similar to modern “warm” mode is marginally convectively unstable under glacial conditions and a relatively small negative perturbation in the freshwater flux to the Nordic Seas can trigger rapid transitions between “cold” and “warm” modes. After being excited, the “warm” mode is metastable on the time scale of a few hundred years. We speculate that the stable “cold” mode corresponds to stadial periods with cold climate over the Northern Atlantic, while temporal transitions between “cold” and “warm” modes could explain the observed Dansgaard-Oeschger oscillations. The warm modern climate does not possess this type of instability, but rapid global warming can trigger a complete collapse of the THC. We discuss the mechanisms and uncertainties of future changes in the THC.

1. Introduction

The understanding that the Earth system, as a complex and strongly nonlinear system, can possess typically nonlinear features, such as multiple equilibria and rapid transitions between them, has become one of the cornerstones of the Earth sciences. The first example of multiple equilibria in the climate system due to positive albedo feedback was demonstrated by Budyko [1969] using an energy balance climate model. Stommel [1961], with a simple box model, found two equilibrium

solutions for the THC. It took several decades before a convincing example of the existence of different climate states for the same external boundary conditions was obtained using complex climate models (AOGCMs). Manabe and Stouffer [1988] with the GFDL coupled climate model found two considerably different climate states, corresponding to two modes of the THC. Paleodata from ice cores and other proxies analyzed in the early nineties [e.g., Dansgaard et al., 1993; Bond et al., 1993] showed numerous and vigorous millennial-scale oscillations of the temperature in the North Atlantic and surrounding areas, indicating the possible relation with the instability of the THC [Broecker, 1994]. This and other results provoked growing interest in the problem of stability and variability of the THC. Furthermore, the results of simulations of future climate change indicated the possibility of a complete collapse of the THC due to global warming and changes in the hydrological cycle [Manabe and Stouffer, 1994]. This finding made the problem of stability of the THC not only of scientific but also of great practical importance.

While the importance of a better understanding of the nonlinear Earth system dynamics in general, and of the THC in particular, became widely recognized, it also became apparent that existing scientific tools were not very suitable to tackle these questions. The typical time scales of the ocean range from a hundred to thousand years, which is at the upper limit of the applicability of GCMs. Some other important processes in the climate system, involving the biosphere, geosphere and cryosphere, have even longer time scales. Simple models, in contrast, can easily operate on these time scales, but the lack of geographical realism (usually they are zonally averaged or box-type models), small number of processes considered, and necessity to make a large number of prescriptions compared to the number of the model's degrees of freedom, limit the usefulness of such models. As a result of these limitations a new class of models, called Earth system models of intermediate complexity (EMICs), appeared aiming to fill the growing gap between simple and complex models. By design EMICs are simpler and more spatially aggregated or coarse-resolution compared to GCMs. This is why they are at least a few orders of magnitude less computationally expensive than GCMs, but being based on an improved understanding of the major processes in the Earth system, these models are able to realistically simulate a considerable number of processes and characteristics. Due to their low computational cost models of intermediate complexity provide a unique opportunity to perform transient paleoclimate simulations on multimillennial and even million-year time scales. In respect of future centennial time-scale climate projections,

EMICs “play” on the same ground as comprehensive climate models, but they are still very useful because they allow us to perform large series of experiments and help to understand the role of different processes, uncertainties and possible reasons for differences between the results of complex models.

2. Model and experimental design

2.1 Model

For the experiments presented here we used Earth system model of intermediate complexity CLIMBER-2 (Version 3). This version is similar to the previous one described in detail in Petoukhov et al. [2000], apart from enhanced horizontal and vertical resolution in the ocean. CLIMBER-2 is a coarse resolution geographically explicit model designed for long-term climate simulations. Geographically the model resolves only individual continents (subcontinents) and ocean basins (Figure 1). Atmosphere, land surface, and vegetation models have the same spatial resolution: 10° in latitude and 51° in longitude. The ocean and sea ice models in longitudinal direction resolve only three ocean basins and in latitudinal direction have a resolutions of 2.5° . Vertically the ocean model has 20 unequal levels with an upper mixed layer of 50m thickness. Each oceanic grid cell communicates with either one, two or three atmosphere grid cells, depending on the width of the ocean basin. Energy, water and momentum exchanges between atmosphere and ocean are calculated on a complementary grid, with a resolution of 2.5° in latitude and 51° in longitude. In latitudinal direction the atmospheric characteristic are interpolated to the ocean grid, while in longitudinal direction (if one ocean grid corresponds to more than one atmosphere grid cell) an additional parameterization is employed to account for the longitudinal gradient of SST due to the ocean gyre circulation.

The atmosphere model POTSDAM (POTsdam Statistical-Dynamical Atmosphere Model) is based on a statistical-dynamical approach and describes the large-scale climatological (i.e. ensemble averaged) dynamics and thermodynamics of the atmosphere. Synoptic process are not described explicitly but instead parameterized in terms of large-scale diffusion with a calculated

diffusion coefficient derived from the theory of baroclinic instability. Dynamics are based on the quasigeostrophic approximation and a special parameterization for the zonally averaged meridional circulation. The model's prognostic equations are derived using an assumption about the universal vertical structure of temperature and humidity. The vertical profile of the temperature is assumed to be linear in the troposphere and specific humidity is exponential with a constant vertical scale. The model employs multilevel radiation schemes for the calculation of short-wave and long-wave radiation fluxes, which take into account two types of clouds (stratus and cumuli), water vapor, carbon dioxide, and aerosols. The model does not resolve the diurnal cycle and has a time step of one day.

Land surface processes are described by the Atmosphere-Surface Interface (ASI) model, which calculates surface fluxes, temperature, soil moisture and snow cover. The model is based on BATS scheme [Dickinson et al., 1986]. Each grid cell is considered as a mixture of up to six different surface types: open ocean, sea ice, forest, grassland, desert and glaciers. The last surface type differs in that it always has the albedo of snow. If the model predicts annual net accumulation of snow at any grid cell, this net accumulation is added to the runoff from this grid cell. The fractions of different vegetation types are calculated using a simple global dynamical vegetation model [Brovkin et al., 1997].

The ocean model is based on the zonally averaged multibasin model of Stocker and Wright [1991]. The meridional component of velocity is calculated in the model via the meridional density gradients and the zonal component of wind stress, computed in the atmosphere module. The ocean is represented by three sectors of variable width, stretching from the North Pole to Antarctica. Within the latitudinal belt where the oceans are separated by continents there is no horizontal mass exchange, while in the Arctic and Southern Oceans the oceanic sectors are connected with each other and the averaged zonal velocity is prescribed. Sea ice is described by a one-layer thermodynamic model with a simple treatment of horizontal advection and diffusion. It predicts thickness and concentration of sea ice. The model does not resolve the gyre circulation, so that meridional heat and salt transports are solely due to the meridional overturning circulation and diffusion, except for the Northern Atlantic, where freshwater transport due to the subpolar gyre circulation is parameterized [see Ganopolski and Rahmstorf, 2001]. The rationale for employing

this parameterization is the following. At present more than half of total surface freshwater to the Arctic and Nordic seas, estimated as 0.18 Sv, escapes from the Arctic via the Canadian archipelago and the East Greenland current in the form of low salinity surface currents (0.08 Sv) and sea ice transport (0.02 Sv) without mixing with the incoming salty Atlantic water [Aagaard and Carmack, 1989]. This helps to sustain convection and to form dense NADW in this area. Since these processes cannot be explicitly described in the zonally averaged ocean model, we implemented special parameterizations for freshwater bypass and ice export. These parameterizations are tuned to produce observed present-day fluxes of freshwater and sea ice and allow us to obtain stability properties of the THC which agree with the results of GCMs.

2.2 Experimental design and background climates

Below we will discuss the stability properties of the THC under two radically different climate conditions: modern and glacial. Under modern climate we understand hereafter equilibrium preindustrial climate state - i.e. climate corresponding to the present-day orbital parameters, preindustrial (280 ppm) CO₂ concentration and potential vegetation cover. To obtain this equilibrium state the model was integrated for 5000 years without using flux correction. This modern climate state simulated by the model is very similar to that described in detail in Petoukhov et al. [2000], where the performance of the previous model version was presented. CLIMBER-2 is able to simulate the spatial and temporal (seasonal) variability of different climatological characteristics in good agreement with empirical data. In particular, the model simulate strong overturning in the Atlantic (Figure 2a) with formation of deep water between 60°N and 70°N.

Glacial climate corresponds to LGM (21 KyBP) boundary conditions. In this case CO₂ concentration was set to 200 ppm, the annual cycle of insolation was changed to that of 21 KyBP, continental ice sheets, their elevation and changes in area of continents were prescribed using the reconstruction of Peltier (1994). The elevation of ice-free land was uniformly increased by 120m and the global salinity increased by 1 p.s.u. to account for sea level drop. For glacial conditions, the efficiency of freshwater bypass was reduced by 50% to take into account the closing of the Canadian archipelago by ice sheets and the partial closure and shallowing of Denmark Strait.

However, this is not crucial for the results. Vegetation cover, as a part of climate system, interactively adjusts to the new climate conditions and produces a positive feedback for global cooling caused by a considerable reduction of forest area [Ganopolski and Claussen, 2000]. The results of the LGM climate simulations in major details agree well with the results of the previous CLIMBER-2 version presented in Ganopolski et al. [1998]. In particular, the new version of the model simulates substantial changes in the THC in the Atlantic - namely a southward shift in the formation area and shallowing of NADW compared to the modern climate (Figure 2d). It is important to stress that the new version has a four-time higher latitudinal resolution in the ocean model, and thus this shift corresponds to 6 grid points and cannot be considered as a numerical artifact of coarse resolution. This southward shift was recently been confirmed in the LGM simulation of the coupled GCM HadCM3 [Hewitt et al., 2001]. These changes in the Atlantic circulations also agree with the results of OGCM simulations performed using surface boundary conditions derived from proxy data [Seidov and Maslin, 1999; Seidov et al., this issue]. Comparison of CLIMBER-2 with the results of LGM simulations performed with different AGCMs [e.g. Kageyama et al., 2001] shows that our results fall within the range of complex climate model simulations and are in agreement with many terrestrial and marine paleodata.

In the last part of the paper we consider future climate change scenarios. In these experiments the model was driven by prescribed CO₂ scenarios. The performance of the model in global warming simulations is described in detail in Ganopolski et al. (2001).

3. Analysis of stability of the ocean thermohaline circulation for different climate states

In general the THC is defined as a component of the ocean circulation which “is driven by changes in sea water density arising from changes in temperature versus salinity” [Houghton et al., 1996] and is complimentary to the wind-driven component of the ocean circulation. In reality, it is difficult to distinguish between these components, since density fields are strongly affected by wind forcing. In a more narrow sense the THC can be defined as a meridional ocean circulation driven by large-scale meridional density gradients. This component of the ocean circulation is

typically depicted by meridional overturning diagrams and is closely linked to the area of deep water formation [Rahmstorf, 1995]. The topology and intensity of this component of the ocean circulation is primarily defined by large scale surface heat and freshwater fluxes. Only this part of the THC can be simulated with the zonally averaged ocean model.

The stability properties of the THC can be presented in the form of stability diagrams (Figure 3). The figure shows the quasi-equilibrium dependence of the intensity of the THC (maximum of meridional overturning) on freshwater flux for modern and glacial conditions. To obtain stability diagrams for different climates we apply a slowly changing freshwater flux anomaly in different regions of the Atlantic ocean similar to Rahmstorf [1996]. The shape of the stability diagram depends on whether freshwater is applied south of the NADW formation area or directly in this area. Otherwise, the results are not very sensitive to the precise position and the details of the applied perturbations. The points E (rectangles) on the stability diagram, corresponding to zero anomalies of freshwater flux, represent the equilibrium THC for unperturbed climate states.

Figure 3 shows that the stability properties of the THC for modern and glacial climates differ considerably. For modern climate, like in Manabe and Stouffer [1988], Stocker and Wright [1991] and Rahmstorf [1996], there are two stable and fundamentally different modes of operation of the THC. The first mode is so-called “conveyor-on” or “warm” mode with deep water formation in the Northern Atlantic (Figure 2a corresponding to point E1 in Figure 3a). Another mode is the “conveyor-off” mode (Figure 2c corresponding to point E2 in Figure 3a). When the freshwater flux to the Atlantic exceeds some critical threshold (point C in Figure 3a) the THC becomes advectively unstable [see Rahmstorf, 2000] and collapses on a time scale of about a thousand years. When freshwater inflow is applied directly in the NADW area the hysteresis loop is narrower because a shutdown (point A) of convection is triggered before the advective stability threshold is reached. The collapse of the THC due to convective instability occurs on a time scale of about a hundred years.

The glacial climate has a rather different shape of the stability diagram (Figure 3b). In this case for unperturbed conditions ($\Delta F_s=0$) there is only one stable climate state corresponding to the “cold” mode of the THC with deep water formation in the area around 50°N. Overturning is shal-

lower than for modern conditions, although its maximum intensity is almost the same. Second, in the case of glacial climate hysteresis behavior is much less pronounced than for the modern climate. Finally, the stability diagram differs not only quantitatively (in respect of the position of transition points between different modes) but also qualitatively between the cases where freshwater flux anomaly is applied north or south of 50°N . When the freshwater flux anomaly is applied southward of 60N (present-day area of deep water formation) the evolution of the THC can be described as a gradual transition between the “cold” and “conveyor-off” modes. Unlike the modern climate Figure 3b does not reveal a clear threshold for the stability of the “cold” mode. With the increase of freshwater flux the overturning becomes weaker and shallower and the area of deep convection migrates to the south. Since this shift in the area of convection leads to a decrease of the density of formed deep water, AABW gradually fills the deep and intermediate Atlantic and the overturning becomes very similar to the modern “conveyor-off” mode (Figure 2c). When the freshwater flux to the Northern Atlantic is decreased, overturning gradually recovers, following almost the same path. If the freshwater flux anomaly is applied north of 50°N , the response of THC is similar to the previous case, but already for a relatively small negative anomaly of the freshwater flux (about -0.02 Sv) deep convection is triggered in the Nordic seas and a transition of the THC occurs from the “cold” glacial mode to a “warm” mode similar to the modern “on” mode of the THC (Figure 2d). This transition is accompanied by a rapid decrease of sea ice cover in the northern Atlantic and an increase of the air temperature over the Atlantic sector in the latitudinal belt between 50N - 70N by more than 6K , and the whole Northern Hemisphere warms by 1K . At the same time, due to the increase of the interhemispheric oceanic heat transport, the Southern Hemisphere is colder in “warm” mode by almost the same amount. When the freshwater flux increases again (i.e., the applied negative anomaly is reduced) transition between “warm” and “cold” modes occurs (point B in Figure 3b) almost for the same negative freshwater flux anomaly as transition A.

The proximity of the points A and B in freshwater space for glacial conditions can be explained by the fact that the width of the hysteresis loop A-B is proportional to the oceanic heat transport, as it is the negative buoyancy flux related to releasing heat to the atmosphere which has to overcome the positive buoyancy flux from freshwater input in this area to sustain convection. For gla-

cial conditions even in the “warm” mode the oceanic heat transport to the Nordic Seas is much smaller than for the modern climate (Figure 4) and this is why the convective hysteresis loop is much narrower in the former case. In the real climate system there are several feedbacks which can additionally affect the stability of the “warm” mode and the width of A-B hysteresis. A transition from the “cold” to the “warm” mode has a pronounced effect on climate over the Laurentide and especially the Fennoscandian ice sheet. An increase of air temperature should increase ablation near the southern margins of these ice sheets and increase the freshwater flux to the northern Atlantic (destabilizing feedback), while an increase of precipitation should lead to an increase of the accumulation at high elevations, and thus at least temporarily increase the freshwater losses from the northern Atlantic (stabilizing feedback). The combined impact of these feedbacks can be time-dependent since ice sheets have long time scales. In the present version of CLIMBER-2 ice sheets are assumed to be in equilibrium and thus these feedbacks are not taken into consideration.

The fact that both points A and B are very close to the unperturbed glacial climate is crucial for the proposed mechanism of rapid glacial climate changes discussed below. This proximity is due to the fact that the terms of the high-latitude freshwater budget, especially runoff, become much smaller in a cold glacial climate, which therefore has a near-zero net freshwater input on the scale of Figure 2. Since modeling of climates considerably different from the present one involves many uncertainties (in particular in defining the boundary conditions and model parameters) and difficulties in the validation of model results, it is important to prove that the results are robust with respect to these uncertainties. One of the possible source of uncertainty is the efficiency of the freshwater bypass (discussed above) during glaciation. To prove that our results are robust with respect to the details of the parameterizations of the freshwater bypass, we performed three additional experiments for glacial conditions. The only differences between these experiments are related to the freshwater bypass parameterizations. In the first experiment (E1) we used the same numerical parameters as for modern conditions; in the second one (E2), both freshwater bypass and ice export parameters were set to one half of their present-day values, and in the third one (E3) both parameterizations were completely switched off. These three experiments cover the whole possible range of uncertainties with respect to freshwater bypass and ice export parameterizations; actually the first and third experiment represent two rather extreme cases. The results of the stability analysis for these experiments are shown in Figure 5. Here, unlike in Figure 3, we

used the annual surface temperature over the northern Atlantic to trace the transition between “cold” and “warm” modes, because this characteristic is the most sensitive measure of these transitions. As seen on Figure 5, the stability diagrams for all three experiments are qualitatively similar, and are characterized by sharp transitions from cold to warm modes (B-transitions). Bifurcation points are shifted between the experiments by values comparable to but smaller than the differences in freshwater transport by the freshwater bypass. The latter is a consequence of the fact that part of the freshwater exported to the south then returns back in the upper ocean layer to the area of convection in the “warm” mode. Both bifurcation points A and B are very close to the “0” perturbation point in experiments E1 and E2, while in the experiment without any export of freshwater (E3) the “cold” mode is more stable and a larger amplitude of negative freshwater forcing is needed to trigger convection in the Nordic Seas. These experiments show that the features shown in Figure 2 are indeed robust. In addition, the sensitivity study showed that the colder the climate, the more the points A and B move to the left, i.e., the more stable the “cold” mode becomes and the larger the freshwater perturbation required to trigger a transition to the “warm” mode. The three qualitatively different circulation modes found in our model coincide with those deduced from paleoclimatic data [Alley et al, 1999] and obtained in OGCM simulations [e.g. Seidov and Maslin, 1999].

Why is the response of the THC to freshwater forcing for glacial condition so robust, and why does the ocean circulation operate in two distinctly different modes? The reason for this discrete structure is the glacial surface freshwater flux, which differs substantially from the present. Figure 6 shows the annual surface freshwater flux into the Atlantic ocean for glacial conditions in comparison with modern conditions. The cold glacial climate is characterized by a strong reduction of precipitation in middle and high latitudes of the Northern Hemisphere [see e.g. Ganopolski et al., 1998]. The reduction of precipitation (directly, and via a reduction of the Eurasian river runoff) as well as an increase of sea ice export from this area lead to a strong decrease of the surface freshwater flux to the Arctic and Nordic seas. At the same time in the latitudinal belt 40-60°N the freshwater flux is higher than at present due to a reduction of evaporation, a southward shift of the storm-track and the melting of sea ice in this area (Figure 6). The reduced ocean meridional heat transport compared to modern conditions cannot sustain deep water formation in this area (area B in Figure 6). Deep convection can operate only either to the south of this area (area A correspond-

ing to the “cold” mode) or to the north (area C corresponding to the “warm” mode). This explains the existence of two distinct modes of operation of the glacial THC. Figure 6 also shows that the contribution to the freshwater flux due to ice export is relatively small compared to background climatological flux. Ice export only reduces the freshwater flux in the Nordic seas and thus makes it easy to trigger convection in the area C, but it does not affect the major features of freshwater forcing. Thus, although freshwater export from the Arctic is important both for the glacial and the modern climate conditions to obtain quantitatively correct stability properties of the THC, qualitatively the results are independent of a specific selection of model parameters.

4. Millennia scale variability of the climate model during glaciation

4.1 Dansgaard-Oeschger events

Previous attempts to understand the mechanisms of rapid climate changes have focused on modelling cold events triggered by freshwater inflow into the North Atlantic [Schiller et al., 1997; Manabe and Stauffer, 1997; Fanning and Weaver, 1997]. All these experiments were performed for modern climate conditions and cannot be directly applied for the explanation of the instability of glacial climate. The results of our simulations suggest that the stability properties of the THC under glacial climate conditions were rather different from the modern. In particular, we have shown that the “cold” mode is the only stable mode of the glacial Atlantic ocean circulation. This implies that cold climate conditions over the northern Atlantic during stadial periods correspond to the normal mode of the glacial THC and do not require additional external forcings for their explanation. The actual problem is to explain the mechanism of “warm” glacial events - Dansgaard-Oeschger events (D/O). Here we speculate that D/O oscillations represent rapid transitions between the “warm” and “cold” modes of the THC, triggered by small variations in freshwater flux to the northern Atlantic.

Spectral time series analysis [Grootes and Stuiver, 1997] of Greenland ice core data reveals a dominant peak at a periodicity of 1470 years associated with the D/O events. A cycle with similar periodicity was also traced in ocean sediments in the northern Atlantic [Bond et al., 1999]. During glaciation this cycle is well correlated with Greenland temperature, but it is also detected during

the Holocene, albeit without a clear counterpart in Greenland temperatures. The mechanism which could cause such a periodicity is still unclear. It was suggested that millennial scale solar variability could be a driving force, but the correlation between solar variability and millennial-scale climate variability is not proven so far. Another possible mechanism, self-sustained oscillation in the climate-ice sheet system, was proposed by Paillard and Labeyrie [1994]. Alley et al. [this issue] speculate that D/O oscillations can be explained by stochastic resonance in the climate system caused by random fluctuations in freshwater flux. The exploration of different mechanisms will be the subject of a forthcoming paper. Here we would merely like to illustrate that a weak periodic freshwater forcing (irrespective of its origin) applied to the high latitudes of the North Atlantic can trigger rapid reorganizations of the Atlantic THC and thereby strong variations in climate consistent with those recorded in paleoclimate proxy data in both hemispheres.

To test this hypothesis, we impose a periodic variation in the freshwater forcing of the Atlantic in the latitude belt 50-70°N (Figure 7a). The amplitude of this forcing is small (0.03 Sv) compared to the other components of the freshwater balance of the Arctic and Nordic seas. The response to the imposed forcing is shown in Fig. 7b-e. During a period of negative anomaly in freshwater, convection is triggered in the area north of 60°N and a transition from the “cold” to the “warm” mode of the THC occurs (transition A in Figure 2b). This transition is accompanied by a vigorous flush in the strength of overturning and an increase of northward oceanic heat and salt transport. Both these factors temporarily stabilize the “warm” mode, which otherwise could not be sustained when the anomaly of freshwater flux is increasing. As the ocean circulation and density gradually (on a time scale of a few hundred years) adjust to each other, overturning is weakening until at some moment the combined effect of a decrease of the oceanic heat transport and an increase of freshwater forcing leads to a complete shut-down of convection in the Nordic Seas and a rapid transition from the “warm” to the “cold” mode of the THC. The time evolution of Greenland temperatures during these warm events has three phases (Figure 7d): an abrupt initial warming on a time scale of a decade, then a gradual cooling trend during five hundred years, terminated by a rapid (about hundred years) temperature drop back to stadial conditions. All these features of simulated warm events resemble the observed D/O events. The region of maximum surface air temperature response is centered on the northern North Atlantic, where temperature changes reach

8°C. This is less than the observed temperature changes in Greenland (up to 15°C, [Dahl-Jensen et al., 1998]), but one has to take into account that the temperature changes shown in Figure 7d represent the average air temperature anomalies over the whole Atlantic sector between 60°N and 70°N, but not the maximum changes which can occur over a smaller area. In Antarctica, temperatures are increasing during the stadial phase and decreasing during the warm event with an amplitude of about 1°C (Figure 7e).

It is important that the characteristics of the simulated D/O events are rather insensitive to the amplitude of the imposed forcing cycle once this amplitude exceeds some critical threshold. To demonstrate this threshold behavior we performed a series of experiments with different parameters for the freshwater bypass described in the previous section. We forced the system with periodic freshwater input with a time-varying amplitude (Figure 8a). As shown in Figure 8b the threshold amplitude depends on model parameters. For both experiments E1 (present day freshwater bypass) and E2 (half of the present day freshwater bypass parameters) the threshold is about 0.02 Sv, while in E3 (no freshwater bypass) full-scale D/O oscillations start only when amplitude of freshwater forcing exceeds 0.05 Sv. When the amplitude is above the threshold, in all experiment the amplitude and the shape of D/O oscillations are very similar and rather insensitive to the amplitude of applied forcing.

4.2 Heinrich events and Bond-cycle

To simulate climate the impact of Heinrich events (large iceberg discharges to the northern Atlantic, [Heinrich, 1988]) a much larger freshwater perturbation with an amplitude of 0.15 Sv and a duration of 2000 years was added to the 1500-year periodic forcing (Figure 9a). This additional perturbation was applied in the same area of the northern North Atlantic as the periodic forcing described above. In response to this freshwater release the conveyor belt gradually shuts down and at the time of maximum freshwater inflow becomes very similar to the modern conveyor-off mode. Since, as seen from Figure 3, the “conveyor-off” mode is not an equilibrium state for unperturbed glacial climate, the THC gradually recovers after the freshwater release starts to decrease. Compared to a stadial mode (cold phase of D/O events), Heinrich events cause only 1-

2°C additional cooling over the northern part of the North Atlantic (Figure 9b), while maximum of cooling is located between 40°N-50°N, where the temperature drops by 4°C. This pattern of climate response to Heinrich events is in agreement with paleo records, which in Greenland show similar stadial temperatures irrespective of the occurrence of Heinrich events, while in mid-latitudes the Atlantic temperature response to Heinrich events is much stronger [Paillard and Cortijo, 1999; Bard et al., 2000]. Compared with D/O oscillations (Figure 7), Heinrich events show a much more pronounced bipolar see-saw [Stocker, 1998] with a strong Antarctic response (2°C warming compared to interstadials). This is due to the larger changes in interhemispheric heat transport and longer duration of these events. In agreement with Blunier et al. [1998] the temperature in Antarctica gradually increases during Heinrich events and decreases during Greenland interstadials.

Although these experiments explain many features of the observed glacial millennial-scale climate variability, there is still one important aspect known from palerecords, which is not captured by the model. Greenland ice cores indicate that a series of warm events always starts after a relatively long cold phases, usually associated with a Heinrich event, and that the series of individual D/O oscillations shows a decline in amplitude and duration (so-called Bond-cycle). This is especially clearly seen between Heinrich events H4 and H2, when the 1500-year cycle is most pronounced in the Greenland ice cores. To simulate these features observed in the paleodata, we superimposed on the freshwater scenario described above a linear trend in freshwater flux of 0.01 Sv/Kyr (Figure 10a). The parameters of the applied freshwater flux were selected in such a way that the total freshwater input between two Heinrich events is equal to zero. This trend could represent either a gradual increase in iceberg discharge from the major ice sheets following a Heinrich event, or a gradual decrease in intensity of the freshwater bypass due to advances of ice sheets and a closing of Denmark Strait. It is also possible that both mechanisms worked together and in the same direction. Figure 10b-e show the temporal response of the Northern Atlantic and Antarctic temperatures to this forcing in comparison with GRIP and BYRD data. A characteristic nonlinear response is seen in the figure. Greenland temperature responds less to the strong Heinrich events than to the much weaker 1500-years forcing. Moreover, it does not respond to each 1500-year cycle, staying longer in the warm mode directly after Heinrich events. Between Heinrich events,

the temperature over the Northern Atlantic shows a pronounced cooling trend. The Antarctic response, in contrast, is much stronger to Heinrich events than to individual D/O events. All these features are consistent with paleodata, showing that changes in freshwater forcing applied only in the Northern Atlantic could fairly realistically explain global-scale changes in temperature. In particular, our results could explain why the Southern Hemisphere appears to lead the Northern Hemisphere by 1-2 kyr, while the driver of these changes is located in the Northern Hemisphere.

5. Centennial time-scale response of thermohaline circulation to the global warming

Based on the past instability of the Atlantic THC and on physical considerations, concerns have been raised that anthropogenic climate change might trigger another instability of the ocean circulation [e.g., Broecker, 1987]. Results of model simulations [Manabe and Stouffer, 1994] have confirmed this possibility. Most simulations performed during the last years with GCMs show a reduction of the strength of the THC during the next century, although they disagree over the amplitude of the changes [e.g., Rahmstorf, 1999]. In particular, a recent experiment with the HadCM-3 coupled model [Wood et al., 1999] shows only moderate reduction in the strength of the THC even for a quadrupling of CO₂ concentration. Dixon et al. [1999] and Mikolajewicz and Voss [2000] analyzed the role of temperature and salinity changes in slowing down the THC and came to qualitatively different conclusions. Simplified models were extensively used to assess uncertainties in the future evolution of the THC. Stocker and Schmittner [1997] studied the critical thresholds for CO₂ concentration and its rate of change beyond which the THC collapses. In Rahmstorf and Ganopolski [1999] we have shown that temperature rise alone only causes a weakening of the THC but cannot lead to a complete shutdown of the ocean conveyor belt. To compare different climate models we proposed a new diagnostic quantity - "North Atlantic hydrological sensitivity" - which is defined as the change in the freshwater flux to the North Atlantic (north of 50°N) per degree of annual warming in the Northern Hemisphere. The long-term evolution of the THC crucially depends on changes in the freshwater flux to the northern Atlantic. If the hydrological sensitivity exceeds some critical value, the THC rapidly collapsed after the year 2100 and a substantial long-lasting cooling over the North Atlantic was simulated. In Ganopolski et al. [2001]

we extended this study by an analysis of different CO₂ scenarios and model parameters. Here we report further global warming experiments with the newest CLIMBER-2 version to analyze the impact of increased freshwater flux to the northern Atlantic and the role of convective and advective instabilities of the THC.

Figure 11 shows results of the model experiments for two standard 1% increase CO₂ scenarios. Comparison of Figures 11b and 11c show that changes in freshwater flux to the northern Atlantic (north of 50°N) are well correlated with a warming in the Northern Hemisphere. The hydrological sensitivity of CLIMBER-2 is 0.013 Sv/K, while the GFDL model has hydrological sensitivity of 0.030 Sv/K. The latest version of the Hadley Centre model, HadCM-3 (Wood et al., 1999), has a hydrological sensitivity 0.020 Sv/K. Moreover, different climate models have a different temperature sensitivity to CO₂. As a result, the total increase of freshwater flux to the northern Atlantic in the GFDL model for the same CO₂ scenario is 3.5 time large than in CLIMBER-2, and in ECHAM-3/LSG model is almost twice as larger [Mikolajewicz and Voss, 2000]. To cover a possible range of uncertainties of the changes in hydrological cycle, we performed experiments with artificially enhanced hydrological sensitivity by applying an additional freshwater flux proportional to the annual warming in the Northern Hemisphere as described in Rahmstorf and Ganopolski [1999]. Although some part of the additional freshwater flux to the northern Atlantic could come from the melting of the Greenland ice sheet and glaciers, the larger part of this increase is due to changes in atmospheric moisture transport. This is why an increase of freshwater flux to the northern Atlantic has to be compensated in the other parts of the oceans. Here we consider two cases: increase of the freshwater input to the northern Atlantic is compensated in the Pacific (1) or in the tropical Atlantic (2). Results of GCM experiments suggest that the second case is more realistic.

The temporal evolution of the Atlantic THC for different CO₂ scenarios and hydrological sensitivities is shown in Figure 11d-f. For convenience we will use acronyms for all these experiments in the form C^kHⁿ, where “C” refers to the CO₂ scenario and “H” refers to the hydrological sensitivity. In these abbreviations k=2 corresponds to a doubling of CO₂ and k=4 to a quadrupling. Index “n” shows the enhancement factor of hydrological sensitivity (compared to CLIMBER-2 hydro-

logical sensitivity). The letter “A” or “P” after this number refers to the area where anomalous flux is compensated (“A” corresponds to the Atlantic, and “P” corresponds to the Pacific). In these abbreviations our standard experiments are denoted as C^2H^1 and C^4H^1 . In the experiments with unaltered hydrological sensitivity (Figure 11d) overturning gradually weakens with the increase of CO_2 and reaches its minimum soon after CO_2 is stabilized. For doubling of CO_2 the model shows a 20% decrease of the THC, and for a quadrupling a 35% decrease. In both cases, after stabilizing of the CO_2 concentration, the THC gradually recovers. If we increase the effective hydrological sensitivity by a factor of four the THC responds strongly to the increase of CO_2 but still survives in a doubling of CO_2 (experiment C^2H^{4A}). In a quadrupling CO_2 experiment (C^4H^{4A}) the THC completely stops after several hundred years. If we compare the differences between compensation of additional freshwater flux in the Atlantic and in Pacific (Figure 11e) then we see that interoceanic transport of moisture is more effective than a redistribution of freshwater within one basin, but there is no qualitative difference between C^4H^{4A} and C^4H^{4P} . The results of experiments C^4H^{3A} and C^4H^{3P} show that the threshold value of the hydrological sensitivity which separates the cases of recovery and shutdown of the THC for a quadrupling CO_2 experiment is close to 0.04 Sv/K.

The rapidity of the shutdown, and the fact that it occurs even if freshwater is only redistributed within the Atlantic, suggests that the convective instability mechanism plays a major role [Rahmstorf et al., 1996]. To test this hypothesis we performed two additional sets of experiments. In the first one, denoted by “U”, the threshold of convective instability was lowered by a reduction of the intensity of the freshwater bypass by a factor of two. In the second one, denoted by “S”, the threshold of convective instability was increased by an increase of the intensity of the freshwater bypass by 50%. Results shown in Figure 11e indicate that during initial phase of the thermohaline slowdown changes in convection do not play an important role and the rate of decline of the THC is almost the same in all experiments. However, the long-term evolution of the THC after stabilization of the CO_2 concentration is different. In experiments with lower stability of convection the THC declines more rapidly and a lower input of freshwater is needed for a complete shutdown. Figure 11e shows that in this case the shutdown of the THC occurs already for a doubled hydro-

logical sensitivity ($C^4H^{2A}(U)$). In the case of more stable convection ($C^4H^{4A}(S)$) the THC starts to rise after stabilization of CO_2 concentration. Thus our results suggest that simulations of rapid changes in the THC need accurate representation of both changes in the freshwater balance of the Northern Atlantic and convective stability properties.

6. Summary and conclusions

Using a climate system model of intermediate complexity we performed a stability analysis of the THC for modern and glacial climate conditions. We show that the stability properties of glacial climate differ fundamentally from those of the modern climate. For modern climate the “warm” and the “off” modes represent the two stable Atlantic circulation states. For glacial condition the situation is rather different. Our stability analysis suggest that the “cold” (stadial) mode represents the only stable mode of the glacial Atlantic ocean circulation, with NADW formation south of Iceland. Another mode of glacial circulation similar to the modern “warm” mode is marginally unstable for glacial conditions. The fact that transitions between “cold” and “warm” modes of the THC can be triggered by small changes in the freshwater flux to the Northern Atlantic is explained by a strong reduction both of the freshwater flux to the Arctic and meridional oceanic heat transport to high latitudes.

Our simulations show that warm events similar to the observed D/O events in time evolution, amplitude and spatial pattern can be triggered in the model as a temporary flip to the “warm” mode with NADW formation in the Nordic Seas. We demonstrated that a weak climate cycle can trigger large-amplitude episodic warm events due to the non-linear threshold response of the Atlantic ocean circulation. The positions of deep water formation areas for “cold” and “warm” modes are separated by a strong maximum in surface freshwater flux and this explains why both transitions are rapid and the amplitude of simulated D/O events is rather insensitive to the details of the model parameterizations and amplitude of applied forcing. Another result of our sensitivity study is that the glacial “cold” mode becomes more stable the colder the climate conditions. This could explain why the THC stays predominantly in the cold mode during the coldest parts of the glacial while D/O events occur almost each 1,500 year cycle during more moderate glacial conditions (50-30 kyr

b.p.).

Heinrich events, simulated in the model as large freshwater pulses, lead to a collapse of NADW formation but no major further cooling in Greenland. The temperature response of Antarctic temperature to Heinrich events is much stronger than to individual D/O events. Both these results are in agreement with the paleoclimatic records. When an additional linear trend is applied to the freshwater flux, the model simulates a sequence of events resembling the one recorded in Greenland and Antarctic ice cores. Thus our results suggest that relatively small variations in freshwater input to the Northern Atlantic could have caused many of the observed features of glacial climate.

Our results suggest that the THC for the modern climate is more stable than for the cold glacial climate with respect to a small perturbation of the freshwater flux, but a sufficiently large perturbation could still destabilize the modern THC and lead to a complete and irreversible shut down of the conveyor belt. The threshold value of the freshwater flux depends on the area where anomalous freshwater flux is applied. This is due to different mechanisms of the instability of the THC.

We performed a series of simulations for two CO₂ scenarios and a range of different hydrological sensitivities. A significant reduction of the strength of the THC in the Atlantic occurs in all experiments. While the initial reduction of the THC is largely due to surface warming, the long-term response of the THC depends on the increase of freshwater flux to the northern North Atlantic. Our results suggest that there is a threshold value of hydrological sensitivity beyond which the Atlantic THC breaks down. The mechanism of rapid (time scale of about one hundred years) collapse of the THC is a convective instability. This is why this threshold value depends on the stability properties of deep convection in the northern North Atlantic. Smaller hydrological sensitivity is needed in the case of reduced export of freshwater from Nordic Seas.

References

- Aagaard, K. and E.C. Carmack, The role of sea ice and other fresh water in the Arctic circulation, *J. Geophys. Res.*, 94, 14,485-14,498, 1989.
- Alley, R.B., P.U. Clark, L.D. Keigwin, and R.S. Webb, Making sense of millennial scale climate change, in *Mechanisms of global climate change at millennial time scales*, edited by P.U. Clark, R.S. Webb, and L.D. Keigwin, pp. 385-394, American Geophysical Union, Washington, D.C., 1999.
- Alley, R.B., S. Anandakrishnan, and P. Jung, Stochastic resonance in the North Atlantic, (this issue), 2001.
- Bard, E., F. Rostek, J.-L. Turon, and S. Gendreau, Hydrological impact of Heinrich events in the subtropical North-east Atlantic, *Science* 289, 1321-1324, 2000.
- Blunier, T., Chappellaz, J. Scwander, A. Dallenbach, B. Stauffer, T.F. Stocker, D. Raynaud, J. Jouzel, H.B. Clausen, C.U. Hammer, and S.J. Johnsen, Asynchrony of Antarctic and Greenland climate change during the last glacial period, *Nature* 394, 739-743, 1998.
- Bond, G., W. Broecker, S. Johnsen, J. McManus, L. Labeyrie, J. Jouzel, and G. Bonani, Correlations between climate records from North Atlantic sediments and Greenland ice, *Nature*, 365, 143-147, 1993.
- Bond, G., W. Showers, M. Elliot, M. Evans, R. Lotti, I. Hajdas, G. Bonani, and S. Johnson, The North Atlantic's 1-2 kyr climate rhythm: Relation to Heinrich events, Dansgaard/Oeschger cycles and the Little Ice Age. in *Mechanisms of global climate change at millennial time scales*, edited by P.U. Clark, R.S. Webb, and L.D. Keigwin, pp. 35-58, American Geophysical Union, Washington, D.C., 1999.
- Broecker, W.S., Unpleasant surprise in the greenhouse? *Nature*, 328, 123, 1987.
- Broecker, W.S., Massive iceberg discharges as triggers for global climate change, *Nature* 372, 421-424, 1994.
- Brovkin, V., A. Ganopolski, and Y. Svirezhev, A continuous climate-vegetation classification for use in climate-biosphere studies, *Ecological Modelling*, 101,251-261, 1997.
- Bryan, F., High-latitude salinity effects and interhemispheric thermohaline circulations, *Nature*, 323, 301-304, 1986.
- Budyko, M.I., The effect of solar radiation variations on the climate of the earth, *Tellus*, 21, 611-619, 1969.
- Daansgard, W., S.J. Johnsen, H.B. Clausen, D. Dahljensen, N.S. Gundestrup, C.U. Hammer, C.S. Hvidberg, J.P. Steffensen, A.E. Sveinbjornsdottir, J. Jouzel, and G. Bond, Evidencies for

- general instability of past climate from a 250-Kyr icecore record, *Nature*, 364, 218-220, 1993.
- Dahl-Jensen, D., K. Mosegaard, N. Gundestrup, G.D. Clow, S.J. Johsen, A.W. Hansen, and N. Balling, Past temperatures directly from the Greenland ice sheet, *Science*, 282, 268-279, 1998.
- Dixon, K.W., T.L. Delworth, M.J. Spelman, and R.J. Stouffer, The influence of transient surface fluxes on North Atlantic overturning in a coupled GCM climate change experiment, *Geophys. Res. Lett.*, 26, 2749-2752, 1999.
- Fannig, A.F., and A.J. Weaver, Temporal-geographical meltwater influence on the North Atlantic conveyor: Implication for the Younger Dryas, *Paleocean.*, 12, 307-320, 1997.
- Heinrich, H., Origin and consequences of cyclic ice rafting in the northeast Atlantic ocean during the past 130,000 years, *Quaternary Res.*, 29, 143-152, 1988.
- Ganopolski, A and M. Claussen, Simulation of Mid-Holocene and LGM climates with a climate system model of intermediate complexity, in *Proceedings of the third PMIP Workshop, WCRP-111*, 201-204, 2000.
- Ganopolski, A., V. Petoukhov, S. Rahmstorf, V. Brovkin, M. Claussen, A. Eliseev, and C. Kubatzki, CLIMBER-2: A climate system model of intermediate complexity. Part II: Model sensitivity. *Clim. Dyn.* (in press), 2001.
- Ganopolski, A., and S. Rahmstorf, Rapid changes of glacial climate simulated in a coupled climate model, *Nature*, 409, 153-158, 2001.
- Ganopolski, A., S. Rahmstorf, V. Petoukhov, and M. Claussen, Simulation of modern and glacial climates with a coupled model of intermediate complexity, *Nature*, 391, 351-356, 1998.
- Grootes, P.M., and M. Stuiver, Oxygen 18/16 variability in Greenland snow and ice with 103- to 105-year time resolution, *J. Geophys. Res.*, 102, 26455-26470, 1997.
- Johsen, S.J., D. Dahl-Jensen, W. Dansgaard, and N. Gundestrup, Greenland paleotemperature derived from GRIP bore hole temperature and ice core isotope profiles, *Tellus*, 47B, 624-629, 1995.
- Hewitt, C.D., A.J. Broccoli, J.F.B. Mitchell, R.J. Stouffer, A coupled model study of the last glacial maximum: Was part of the North Atlantic relatively warm? *Geophys. Res. Lett.*, 2001 (in press).
- Houghton, J.T., L.G. Meira Filho, B.A. Callander, N. Harris, A. Kattenberg, K. Maskell, *Climate Change 1995 - The science of climate change*, Cambridge University Press, 572 pp, 1996.
- Kageyama, M., O. Peyron, S. Pinot, P. Tarasov, J. Guiot, S. Joussame, and G. Ramstein, The Last Glacial Maximum climate over Europe and western Siberia: a PMIP comparison between models and data, *Clim. Dyn.*, 17, 23-43, 2001

- Manabe, S., and R.J. Stouffer, Two stable equilibria of a coupled ocean-atmosphere model, *J Climate*, 1, 841-866, 1988.
- Manabe, S., and R.J. Stouffer, Multiple-century response of a coupled ocean-atmosphere model to an increase of atmospheric carbon dioxide, *J., Climate*, 7, 5-23, 1994.
- Mikolajewicz, U., and R. Voss, The role of the individual air-sea flux components in CO₂-induced changes of the ocean's circulation and climate. *Clim. Dyn.*,16, 627-642, 2000.
- Paillard, D., and E. Cortijo, A simulation of the Atlantic meridional circulation during Heinrich event 4 using reconstructed sea surface temperatures and salinities, *Paleoceanography*, 14, 716-724, 1999.
- Paillard, D., and L. Labeyrie, Abrupt climate warming after Heinrich events: the role of the thermohaline circulation, *Nature*, 372, 162-164, 1994.
- Petoukhov, V., A. Ganopolski, V. Brovkin, M. Claussen, A. Eliseev, C. Kubatzki, S. Rahmstorf, CLIMBER-2: a climate system model of intermediate complexity. Part I: Model description and performance for present climate, *Clim. Dyn.*, 16, 1-17, 2000.
- Rahmstorf, S., Bifurcations of the Atlantic thermohaline circulation in response to changes in the hydrological cycle, *Nature*, 378, 145-149, 1995.
- Rahmstorf, S., On the freshwater forcing and transport of the Atlantic thermohaline circulation, *Clim. Dyn.*, 12, 799-811, 1996.
- Rahmstorf, S., Shifting seas in greenhouse? *Nature*, 399, 523-524, 1999.
- Rahmstorf, S., The thermohaline ocean circulation: a system with dangerous thresholds? *Climatic Change*, 46, 247-256, 2000.
- Rahmstorf, S., and A. Ganopolski, Long-term global warming simulations with efficient climate model, *Climatic Change*, 43, 353-367, 1999.
- Rahmstorf, S., J. Marotzke, and J. Willebrand, Stability of the thermohaline circulation, in *The warm water sphere of the North Atlantic ocean*, edited by W. Krauss, Borntraeger, Stuttgart, pp. 129-158, 1996.
- Schiller, A., U. Mikolajewicz, and R. Voss, The stability of the North Atlantic thermohaline circulation in a coupled ocean-atmosphere general circulation model, *Clim. Dyn.*, 13, 325-347, 1997.
- Seidov D., B. J. Haupt, E. Barron, and M. Maslin, Ocean bi-polar seesaw and climate: southern versus northern meltwater impact, (this issue), 2001.

- Seidov, D., and M. Maslin, North Atlantic deep water circulation collapse during Heinrich events, *Geology*, 27, 23-26, 1999.
- Stocker, T.F., The seesaw effect, *Science* 282, 61-62, 1998.
- Stocker, T., Past and future reorganisations in the climate system, *Quatern. Sci. Rev.*, 19, 301-319, 2000.
- Stocker, T.F., and A. Schmittner, Influence of CO₂ emission rates on the stability of the thermohaline circulation, *Nature*, 388, 862-865.
- Stocker, T.F., and D.G. Wright, Rapid transitions of the ocean's deep circulation induced by changes in surface water fluxes, *Nature*, 351, 729-732, 1991.
- Stocker, T.F., and D.G. Wright, A zonally averaged ocean model for the thermohaline circulation. Part II: Interocean circulation in the Pacific Atlantic basin system, *J. Phys. Oceanogr*, 21, 1725-1739, 1991.
- Stommel, H.M., Thermohaline convection with two stable regimes of flow. *Tellus*, 13, 529-541, 1961.
- Wood, R., A. Keen, J.F.B. Mitchel, and J.M. Gregory, Changing spatial structure of the thermohaline circulation in response to atmospheric CO₂ forcing in a climate model, *Nature*, 399, 572-575, 1999.

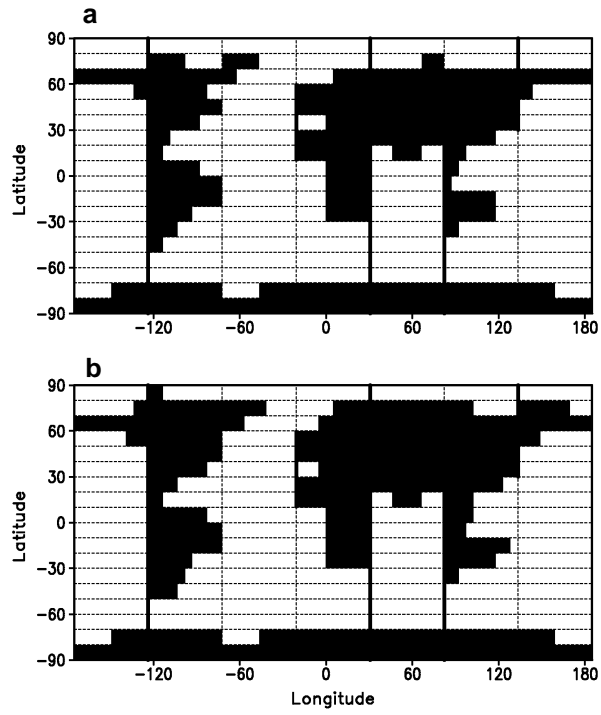


Fig. 1 Representation of the Earth's geography in the model for modern conditions (a) and glacial conditions (b). The black area represents the areas of land. Dashed lines show the atmospheric grid, solid lines separate ocean basins.

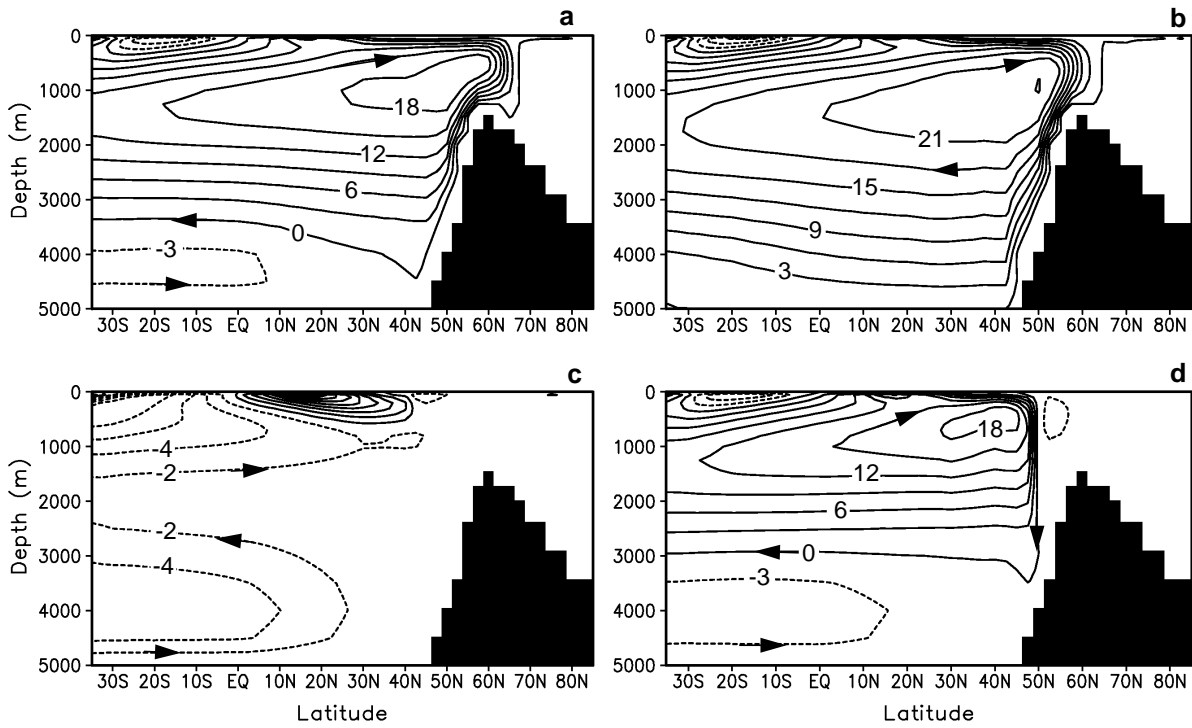


Fig. 2 Modes of Atlantic THC in the coupled model. (a) Holocene warm mode. (b) Glacial warm (or interstadial) mode. (c) Holocene "off" mode. (d) Glacial "cold" (stadial) mode. Figure from Ganopolski and Rahmstorf (2001).

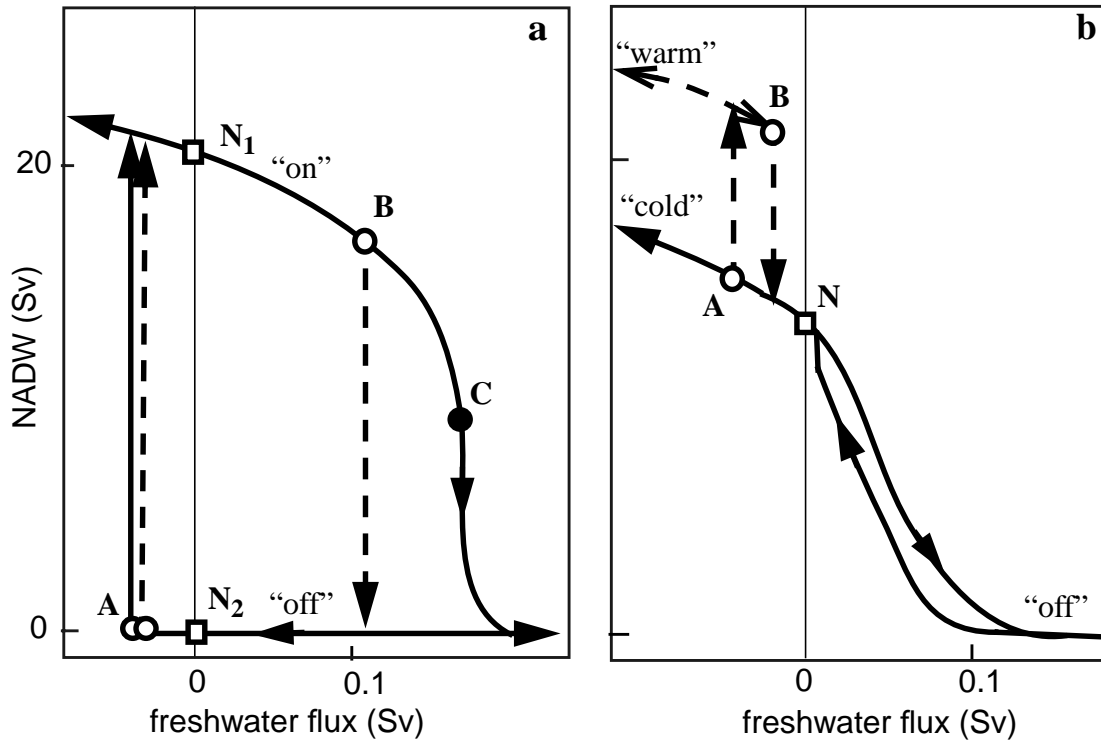


Fig.3. Schematic stability diagram for the Atlantic thermohaline circulation for the present climate (a) and the glacial climate (b) based on Ganopolski and Rahmstorf (2001). Solid lines correspond to freshwater perturbation added in the latitude belt 20° - 50° N, and dashed lines - in the latitude belt 50° - 70° N. Points N represent the equilibrium climate states for unperturbed conditions. C is a bifurcation point for advective instability. Points A and B represent transitions between “on” and “off” modes for present climate and between “warm” and “cold” for glacial climate due to start-up and collapse of convection in the Nordic Seas.

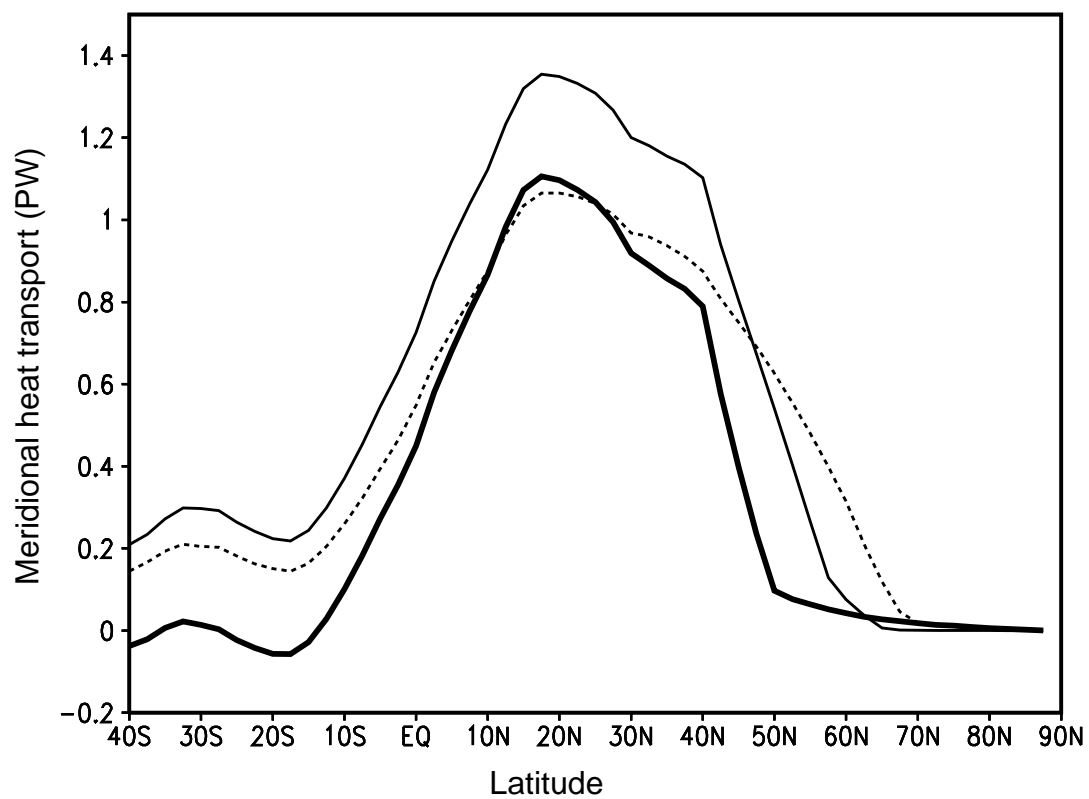


Fig. 4 Meridional heat transport in the Atlantic. Glacial cold mode - thick solid line; glacial warm mode - thin solid line; present-day climate - dashed line.

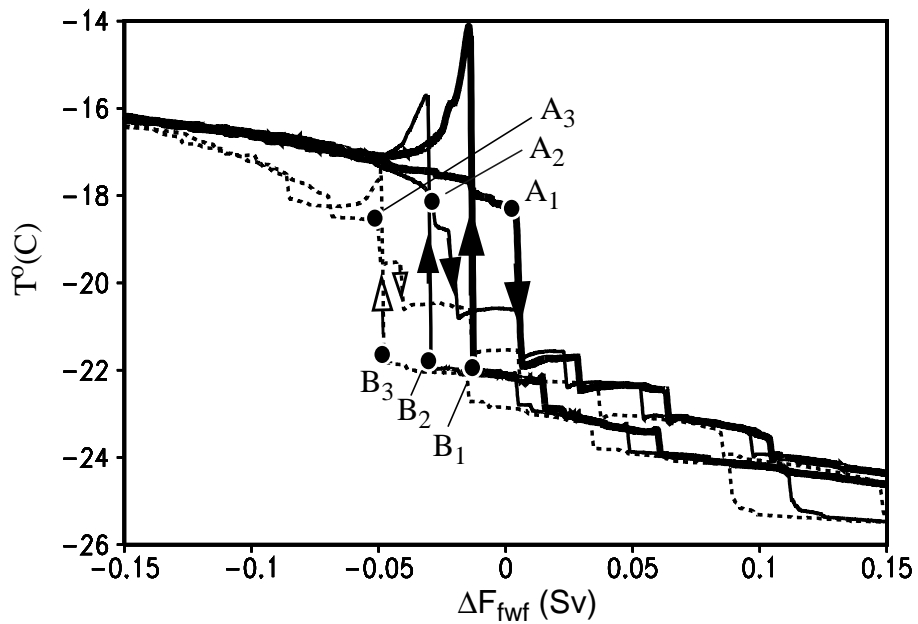


Fig. 5 Stability diagram for glacial conditions in terms of North Atlantic sector air temperature (60° - 70° N). The thick solid line corresponds to the experiment with present parameters of the freshwater bypass, thin solid line - parameters of the freshwater bypass are half of present values, dashed line - without freshwater bypass. Dots indicate the positions of convective transitions from “warm” to “cold” (A) and from “cold” to “warm” (B) modes.

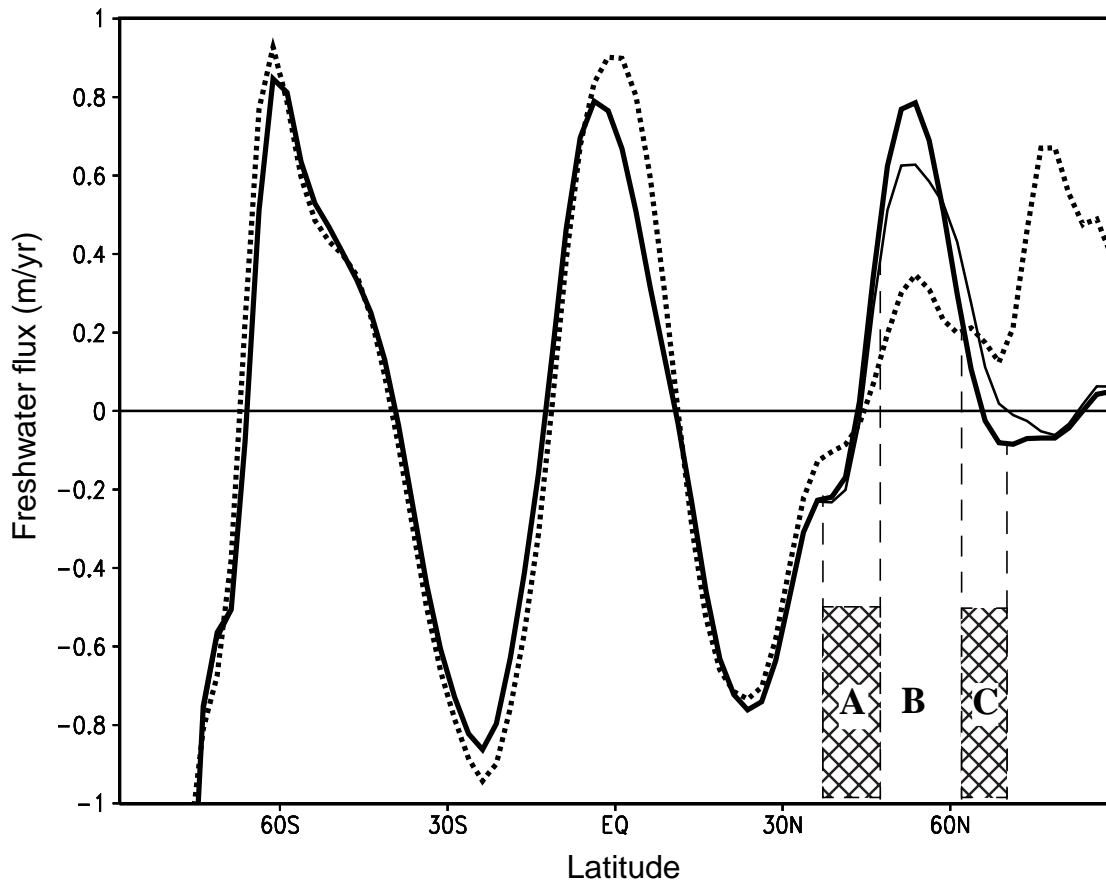


Fig. 6 Annual surface freshwater flux into the Atlantic sector for glacial (solid lines) and modern (dashed line) conditions. These fluxes include precipitation, evaporation, runoff and melting/freezing of ice (i.e. explicitly include effect of ice export parameterization but not effect of freshwater bypass since the latter is treated as advective flux). Thick lines correspond to standard model set-up; thin line corresponds to an experiment in which freshwater bypass parameterizations were switched off. The strong maximum in the Arctic for modern conditions is due to Eurasian rivers runoff.

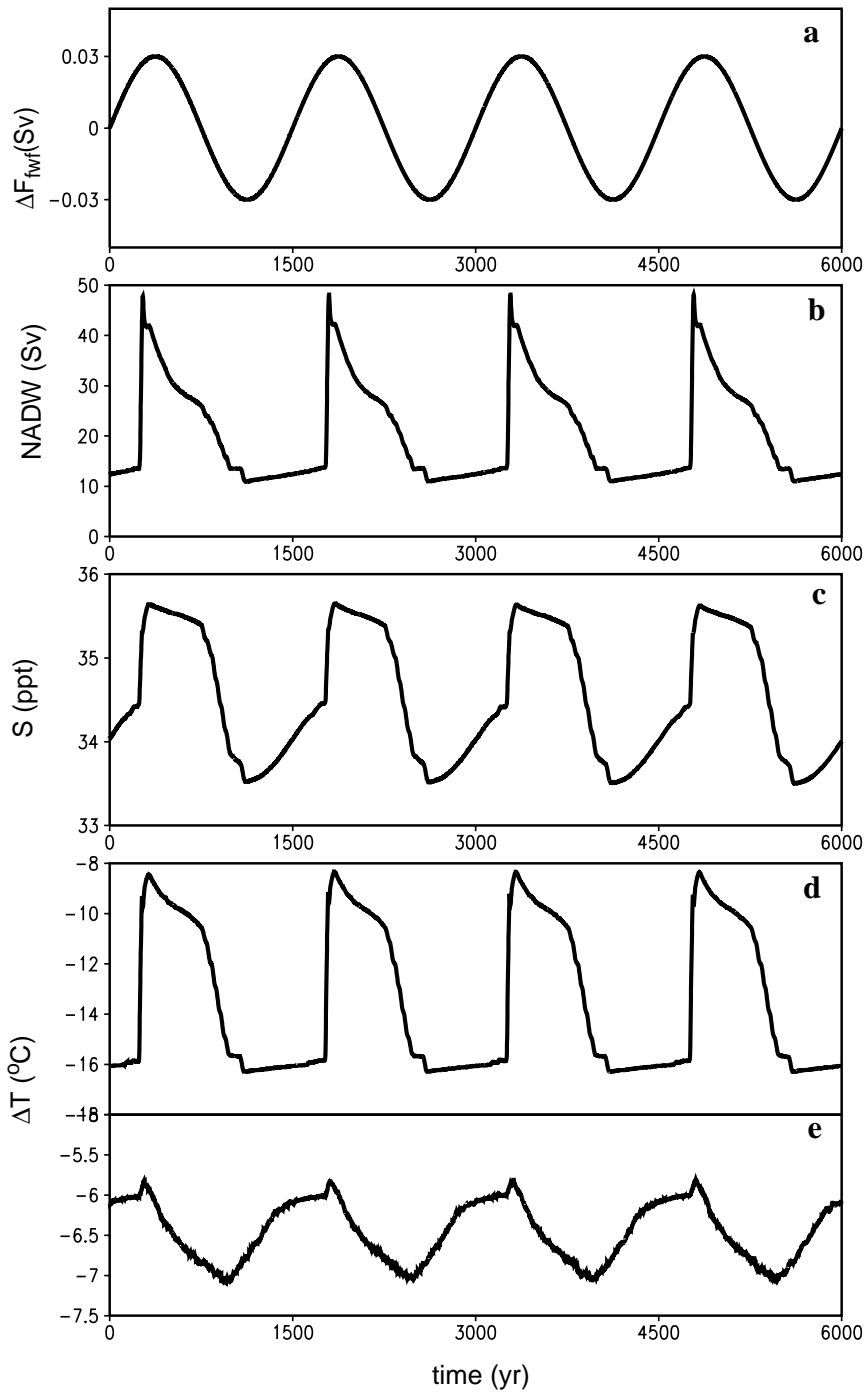


Fig. 7. Simulated D/O events. (a) Forcing, (b) Atlantic overturning, (c) Atlantic salinity at 60°N , (d) air temperature in the northern North Atlantic sector (60° - 70°N), and (e) temperature in Antarctica (temperature values are given as the difference to the present-day climate).

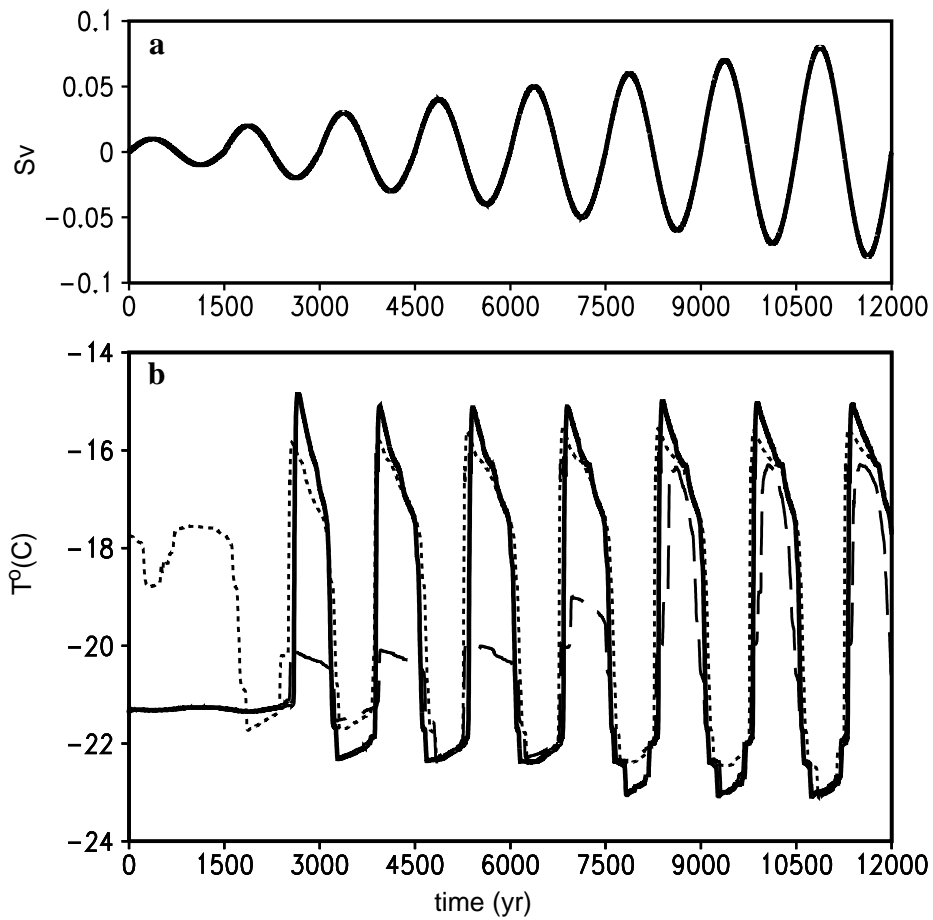


Fig. 8. Triggering of rapid changes by freshwater forcing of variable amplitude. (a) Forcing, (b) air temperature in the northern North Atlantic sector (60° - 70° N). The dotted line corresponds to the experiment with present parameters of the freshwater bypass (E1), the thick solid line - parameters of the freshwater bypass are half of present values (E2), the dashed line - without freshwater bypass (E3).

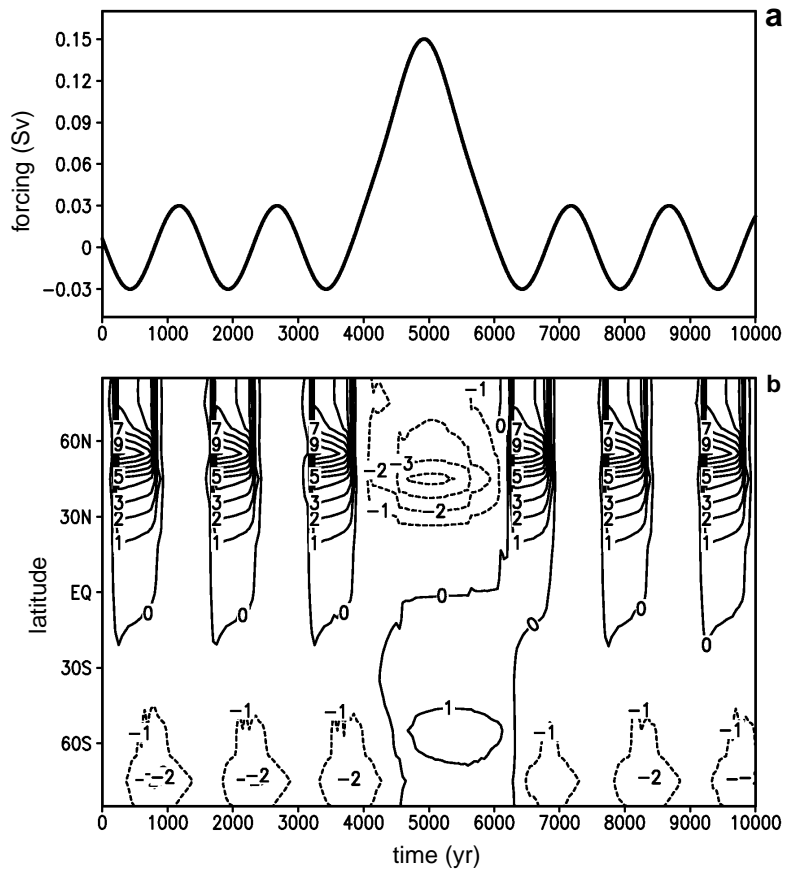


Fig. 9. Simulated D/O events and Heinrich event. (a) Forcing, (b) annual surface air temperature anomalies (differences from equilibrium LGM state) for the Atlantic sector.

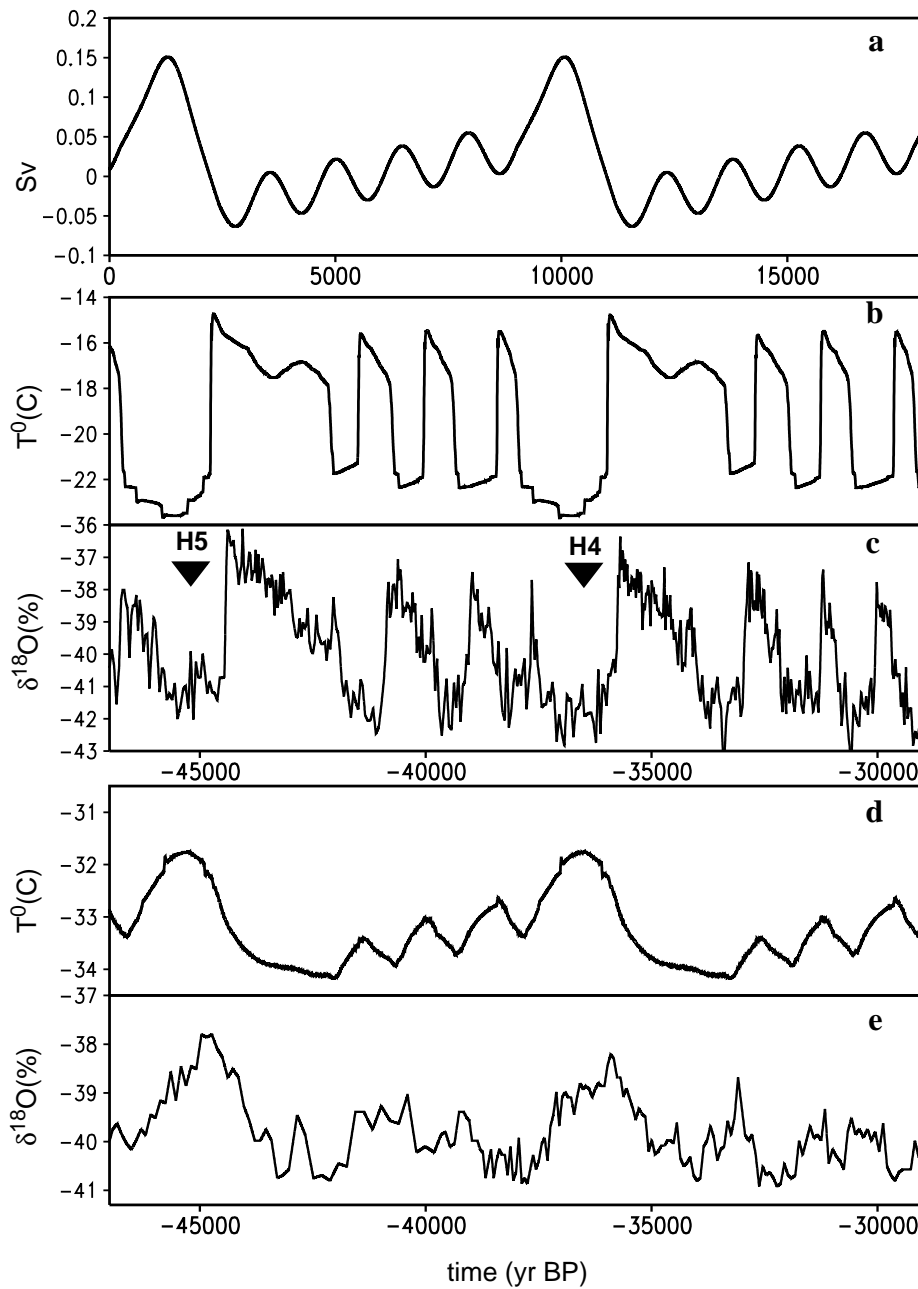


Fig. 10. Simulated Bond cycle in comparison with paleoclimatic records. (a) Freshwater forcing, (b) air temperature in the northern North Atlantic sector (60° - 70° N), (c) GRIP $\delta^{18}\text{O}$ data (Johnsen et al, 1995), (d) temperature over Antarctica, (e) Byrd $\delta^{18}\text{O}$ data (Blunier et al., 1998).

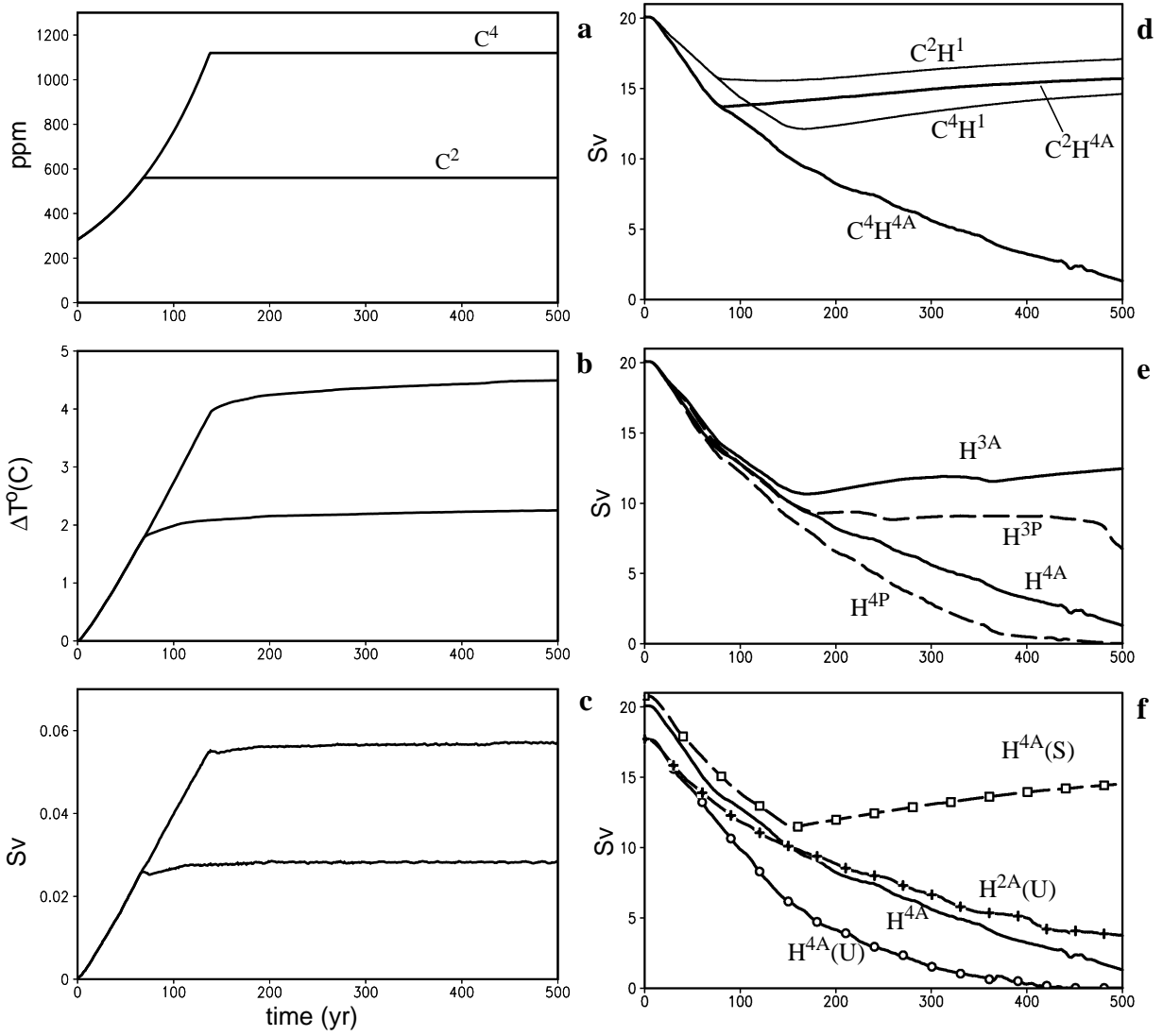


Fig. 11 Time series of forcing scenarios and model variables. (a) CO₂ scenarios; (b) Northern Hemisphere temperature changes; (c) model simulated changes in freshwater flux to the Northern Atlantic; (d-e) NADW. Thin solid lines on (d) correspond to the standard runs, thick solid lines on (d-f) correspond to experiments with “Atlantic compensation” and dashed lines correspond “Pacific compensation”. Only CO₂ quadrupling experiments (C⁴ experiments) are shown in (e) and (f), this is why the first index in experiment’s acronyms is omitted in these figures.